

Thermal echo in a finite one-dimensional harmonic crystal

A.S. Murachev,^{*} A.M. Krivtsov,[†] and D.V. Tsvetkov[‡]

Department of Theoretical Mechanics, Peter the Great St. Petersburg Polytechnic University

(Dated: 02 July 2018)

An instant homogeneous thermal perturbation in the finite harmonic one-dimensional crystal is studied. Previously it was shown that for the same problem in the infinite crystal the kinetic temperature oscillates with decreasing amplitude described by the Bessel function of the first kind. In the present paper it is shown that in the finite crystal this behavior is observed only until a certain period of time when a sharp increase of the oscillations amplitude is realized. This phenomenon, further referred to as the thermal echo, is realized periodically, with the period proportional to the crystal size. The amplitude for each subsequent echo is lower than for the previous one. It is obtained analytically that the time-dependance of the kinetic temperature can be described by an infinite sum of the Bessel functions with multiple indexes. It is also shown that the thermal echo in the thermodynamic limit is described by the Airy function.

I. INTRODUCTION

Analytical and experimental results demonstrate an anomalous nature of thermal processes in ultrapure materials [1–9]. These processes can be caused by shock waves [10–13] or by ultrashort laser pulses [14–20]. One-dimensional crystal lattices are subject of an extensive research since they admit analytical solutions and allow verification of fundamental phenomena inherent also for higher dimensional systems [21–25]. An analytical description of the thermal processes in non-equilibrium harmonic crystals can be obtained on the basis of the covariance analysis [1, 3, 4, 26]. The corresponding description of the anomalous heat propagation is presented in papers [3, 27, 28] for one dimension and in works [4, 29–31] for two and three dimensions.

One of the specific phenomena of the nonequilibrium thermal processes in discrete molecular systems are the high-frequency oscillations of the kinetic temperature, which have long been known from the results of numerical simulation [32]. Covariance analysis admit analytical description of this phenomenon, for example in the case of the instantaneous heat perturbation of the simplest model of one-dimensional harmonic crystal these oscillations are described by the Bessel function of the first kind and the zero order [26], similar result was obtained earlier by direct analytical solution of the equations of the atoms motion by Ilya Prigogine [33]. For the case of the one-dimensional crystal on an elastic substrate the same problem is solved in [24], for higher dimensions in papers [4, 30].

Unlike previous papers [3, 24, 26, 27], where the main attention is focused on infinite crystals, the present paper investigates thermal processes in *finite* crystals [34]. The systems with a finite number of particles is of practical importance, especially because nanotechnologies are

actively developing [35–39]. In the current paper it is demonstrated that for the finite crystals the oscillation amplitude is decreasing only until a certain moment of time when a sharp increase of the amplitude of the kinetic temperature oscillations is realized. This phenomenon can be interpreted as a thermal echo, which will be analyzed in details in the presented paper. Exact and asymptotic formulas describing the oscillations of the kinetic temperature will be obtained. These results, in particular, are important for description of the anomalous heat propagation in ultrapure materials [3, 5, 40].

II. DYNAMICS OF THE CRYSTAL

A. The mathematical model

We consider a one-dimensional harmonic crystal containing N particles connected by harmonic springs. The equation of motion for the particles is

$$\ddot{u}_k = \mathcal{L}u_k, \quad \mathcal{L}u_k \stackrel{\text{def}}{=} \omega_e^2(u_{k+1} - 2u_k + u_{k-1}), \quad (1)$$

where u_k is the displacement of the k^{th} particle ($k = 1..N$), \mathcal{L} is the linear difference operator, $\omega_e = \sqrt{C/m}$ is the elementary frequency, C is the stiffness of the interparticle bond, m is the particle mass. Periodic boundary conditions are used:

$$u_0 \stackrel{\text{def}}{=} u_N, \quad u_{N+1} \stackrel{\text{def}}{=} u_1. \quad (2)$$

The initial conditions are

$$u_k = 0, \quad v_k \stackrel{\text{def}}{=} \dot{u}_k = \sigma \rho_k, \quad (3)$$

where ρ_k are independent random numbers with zero mathematical expectation and unit variance, σ is the initial velocity variance. These initial conditions correspond to an instantaneous temperature perturbation, such as perturbations caused by an ultrashort laser pulse [14, 15, 17].

The initial problem (1)–(3) describes stochastic dynamics of the particles in the crystal. Further the deterministic equations for the statistical characteristics of

^{*} andrey.murachev@gmail.com

[†] akrivtsov@bk.ru

[‡] dvtsvetkov@ya.ru

motion (covariances) are analyzed to describe the thermal processes in the crystal.

B. The dynamics of covariances

One of the key statistical characteristics of the crystal is the kinetic temperature T , which can be determined by the mathematical expectation $\langle \dots \rangle$ of the square of the centered velocity. The corresponding formula for a one-dimensional case is

$$T = \frac{m}{k_B} \langle \tilde{v}_k^2 \rangle, \quad (4)$$

where

$$\tilde{v}_k \stackrel{\text{def}}{=} v_k - \bar{v}, \quad \bar{v} \stackrel{\text{def}}{=} \frac{1}{N} \sum_{k=0}^{N-1} v_k. \quad (5)$$

Here \bar{v} is the center of mass velocity and k_B is the Boltzmann constant. In order to obtain a closed system of equations for statistical characteristics it is imperative that we consider the covariances of the particle velocities [3, 26, 30]:

$$\kappa_n = \langle \tilde{v}_k \tilde{v}_{k+n} \rangle, \quad (6)$$

which are the quantities characterizing motion of the particle pairs. The following initial problem for the velocity covariances can be obtained by differentiating the covariances using relations (1)–(3) (see Appendix A):

$$\begin{aligned} \ddot{\kappa}_n - 4\mathcal{L}\kappa_n &= -2\mathcal{L}\kappa_n^0, \\ t = 0: \quad \kappa_n = \kappa_n^0 &\stackrel{\text{def}}{=} \sigma^2 \delta_n^N - \frac{\sigma^2}{N}, \quad \dot{\kappa}_n = 0, \end{aligned} \quad (7)$$

where δ_n^N is the periodical Kronecker symbol: $\delta_n^N = 1$ for n divisible by N (including $n = 0$), otherwise $\delta_n^N = 0$. Additionally the covariances satisfy the periodicity conditions: $\kappa_{n+N} = \kappa_n$. After solving the initial problem (7), the kinetic temperature of the crystal can be found using formula (4), which can be written as

$$T = \frac{m}{k_B} \kappa_n \Big|_{n=0}. \quad (8)$$

C. Representation via Bessel functions

Solution of the initial problem (7) yields the following expression for the temperature of the crystal (see Appendix B)

$$T = \frac{\Delta T}{2} \left(1 + \frac{1}{N} \sum_{k=1}^{N-1} \cos \left(4\omega_\epsilon t \sin \frac{\pi k}{N} \right) \right), \quad (9)$$

where

$$\Delta T = \frac{m}{k_B} \kappa_n^0 \Big|_{n=0} \quad (10)$$

is the temperature jump initially caused by the thermal perturbation. This expression accurately describes the time dependence of the kinetic temperature of the harmonic crystal after an instant thermal perturbation. Formula (9) can be effectively used for computations, however it is less appropriate for an analytical analysis. Therefore an alternative representation for the crystal temperature in terms of the Bessel functions is obtained below.

Let us consider identity [41]

$$\cos(z \sin \vartheta) = \sum_{p=-\infty}^{\infty} J_{2p}(z) \cos(2p\vartheta), \quad (11)$$

where $J_{2p}(t)$ is the Bessel function of the first kind of order $2p$. Substitution $\vartheta = \pi k/N$ and summation over k yields

$$\frac{1}{N} \sum_{k=0}^{N-1} \cos \left(z \sin \frac{\pi k}{N} \right) = \sum_{p=-\infty}^{\infty} J_{2p}(z) \delta_p^N, \quad (12)$$

where

$$\delta_p^N = \frac{1}{N} \sum_{k=0}^{N-1} \cos \left(p \frac{2\pi k}{N} \right). \quad (13)$$

As mentioned before, $\delta_p^N = 1$ if p is divisible by N , otherwise $\delta_p^N = 0$. Identity (13) is derived in appendix C. Using properties of δ_p^N formula (12) can be reduced to

$$\frac{1}{N} \sum_{k=0}^{N-1} \cos \left(z \sin \frac{\pi k}{N} \right) = \sum_{p=-\infty}^{\infty} J_{2pN}(z). \quad (14)$$

Substitution of the obtained formula to expression (9) gives

$$T = T_E + \frac{\Delta T}{2} \sum_{p=-\infty}^{\infty} J_{2pN}(4\omega_\epsilon t), \quad (15)$$

where

$$T_E \stackrel{\text{def}}{=} \frac{\Delta T}{2} \left(1 - \frac{1}{N} \right) \quad (16)$$

is an equilibrium temperature [?]. Using identity $J_{-\mu} \equiv J_\mu$ formula (15) can be rewritten as

$$T = T_E + \frac{\Delta T}{2} J_0(4\omega_\epsilon t) + \Delta T \sum_{p=1}^{\infty} J_{2pN}(4\omega_\epsilon t). \quad (17)$$

Thus, the kinetic temperature can be represented as the equilibrium temperature plus the sum of terms proportional to the Bessel functions of multiple orders.

Both expressions (9) and (17) are accurate, but expression (17) is more suitable for the analytical analysis. Indeed, for a positive integer index μ the Bessel function

$J_\mu(x)$ is almost zero for all positive x up to a vicinity of the point $x = \mu$. Therefore, for a finite moment in time only a finite number of terms give noticeable contribution to representation (17). For illustration let us consider series

$$S(x) = J_0(x) + 2J_\mu(x) + 2J_{2\mu}(x) + \dots + 2J_{p\mu}(x) + \dots \quad (18)$$

Graphs for $S(x)$ and the first three terms of its representation (18) are shown in Fig. 1. The figure shows that for almost [?] the entire interval $[0, \mu]$ the sum $S(x)$ is determined only by the first term in expression (18). Similarly, for almost the entire interval $[\mu, 2\mu]$ the sum $S(x)$ is determined by the first two terms, and so on.

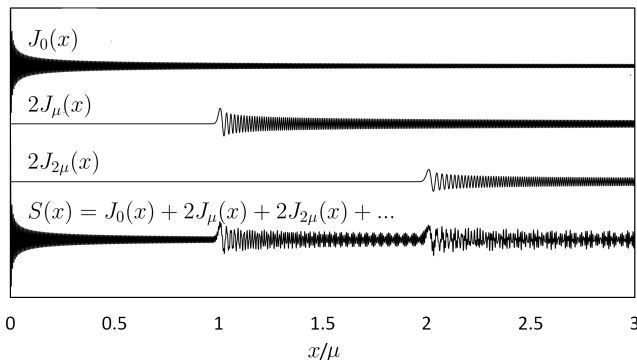


FIG. 1. Bessel functions with indices multiple of $\mu = 10^3$ (the top three graphs); sum of the Bessel functions (the lower graph).

If the crystal has a nonzero initial temperature T_0 before the heat perturbation then the equilibrium temperature (16) contains additional term T_0 :

$$T_E = T_0 + \frac{\Delta T}{2} \left(1 - \frac{1}{N} \right), \quad (19)$$

while expressions (15), (17) remain unchanged. This is a direct consequence of the superposition principle, which is valid for harmonic systems.

$$\begin{aligned} \tilde{T} &= T - T_E = \\ &= \frac{\Delta T}{2} \left(J_0(4\omega_e t) + 2 \sum_{p=1}^{\infty} J_{2pN}(4\omega_e t) - \frac{1}{N} \right), \end{aligned} \quad (20)$$

where ΔT is the temperature jump [?], is caused by temperature perturbation and $T_E \stackrel{\text{def}}{=} T_0 + \Delta T/2$ is the equilibrium temperature. As follows, from expression (20) the equilibrium temperature is the temperature reached when $N \rightarrow \infty$, $t \rightarrow \infty$ (equilibrium state of an infinite crystal).

III. OSCILLATIONS OF THE KINETIC TEMPERATURE

A. Thermal echo

According to the virial theorem [42, 43] in harmonic systems a time average for both kinetic and potential energies tends to the same value. Earlier studies [26, 33] have shown that in the one-dimensional infinite harmonic crystal this equilibration process is accompanied by the energy (and, consequently, the temperature) oscillations described by the Bessel function of the zero order. According to formula (15) or (17) the same process in the finite harmonic crystal is described by an infinite series of the Bessel functions with multiple orders.

This phenomenon can be explained as follows. The solution of the initial problem (1)–(3) due to the linearity of the system can be represented as a superposition of N problems for each individual particle, where only this certain particle was randomly disturbed. For each particle elastic waves propagate to the right and left from its position in the crystal and superposition of these waves for all particles describes the thermal process in the crystal. Since the crystal is periodic (circular), the elastic waves meet each other after they have passed half-length of the crystal. All particles were disturbed instantly, therefore the waves initiated from each particle meet simultaneously, causing a sharp short-term increase of the system's kinetic temperature — the first thermal echo. Then the waves travel further and meet again — the second thermal echo is realized, and so on. Each thermal echo (17) is expressed in terms of the Bessel functions of order $2pN$, where $p = 1, 2, 3, \dots$ is the echo number.

The crystal is discrete system that possesses dispersion — the wave speed depends on the wave length. The fastest are the long waves that travel with the speed of sound $c_s = a\omega_e$ [44, 45], where ω_e is an elementary frequency (1), a is the lattice step. These waves meet after they pass half-length of the crystal, therefore the thermal echo period is

$$\tau_0 = \frac{L}{2c_s} = \frac{N}{2\omega_e}, \quad (21)$$

where $L = Na$ is the crystal length. Shorter waves are slower and meet later — therefore the thermal echo has a finite width, and consequently each next thermal echo is less prominent.

The time $t = p\tau_0$ we will call the reference time for the thermal echo number p . At that time the long waves from the initial disturbances have the meeting number p , that causes the temperature oscillations of corresponding the thermal echo.

B. Thermal echo implementations

Using formula (17) the kinetic temperature can be represented in the form:

$$T = T_E + T_B + T_1 + T_2 + \dots + T_p + \dots; \quad (22)$$

$$T_B = \frac{\Delta T}{2} J_0(4\omega_e t), \quad T_p = \Delta T J_{2pN}(4\omega_e t);$$

where T_E is the equilibrium temperature (17), T_B is the basic thermal mode, and the subsequent terms T_p are the thermal modes with the number $p = 1, 2, 3, \dots$

The temperature oscillations in a crystal containing 10^6 particles are shown in Fig. 2. The graphs show the time vicinity of the first, second and third thermal echo. The first thermal echo is initiated for $t \approx \tau_0$. The corresponding temperature oscillations (22) are described by the first thermal mode T_1 .

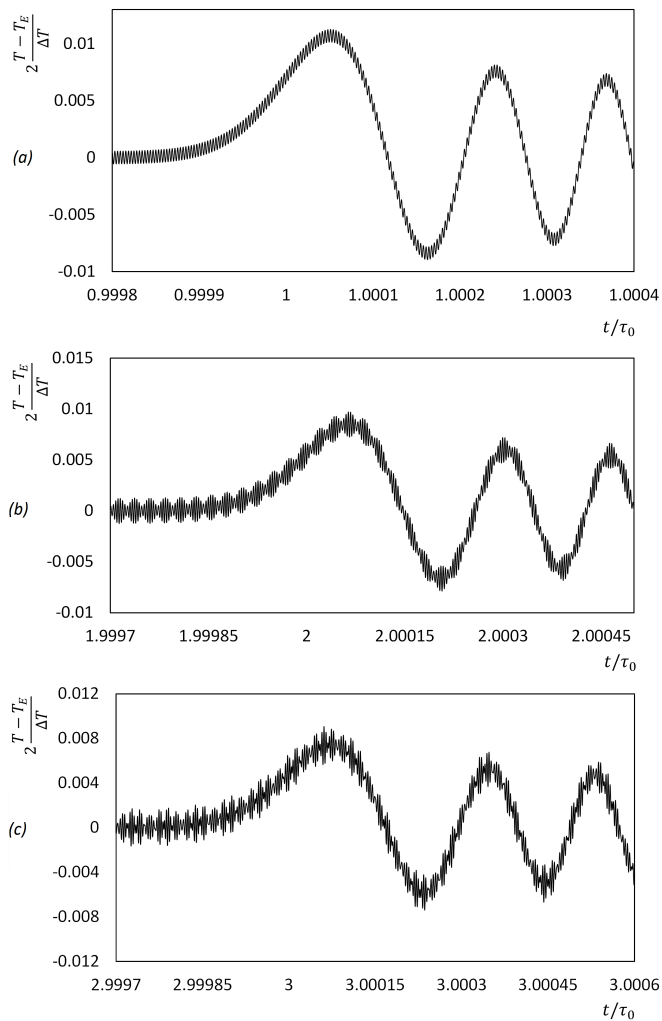


FIG. 2. Beats of temperature. The number of particles $N = 10^6$, T_E is the equilibrium temperature, ΔT is the temperature jump of the crystal caused by the thermal perturbation, t is time, τ_0 is the period of realization of the thermal echo.

Each thermal mode is representing by the corresponding Bessel function. Bessel functions are not periodic, however it is convenient to consider a quasiperiod — the interval between two consequent maximums of the Bessel function. This quasiperiod is not a constant, its value decreases for each next maximum.

As can be seen from Fig. 2 (a), for $t \approx \tau_0$ the oscillations are superposition (17) of the basic mode T_B (small short oscillations on the graph) and the first mode T_1 (global oscillations on the graph). For $t \approx \tau_0$ the quasiperiod of the basic mode is much smaller than the quasiperiod of the first mode. The larger is the crystal, the more significant is the discrepancy. For times $t \approx 2\tau_0$, the oscillation parameters of the basic and the first thermal modes become close, which leads to a beat phenomena. For $t \approx 2\tau_0$, the second thermal echo is realized, superimposed by the mentioned beatings — see Fig. 2 (b). For $t \approx 3\tau_0$, the third thermal echo is realized (see Fig. 2 (c)). Numerical experiments show that for large times plural realizations of the thermal echo result in an increasingly complex form of beats. The realizations of the thermal echo with large ordinal numbers is less pronounced against the background of residual oscillations from previous implementations of the thermal echo. As a result, at large times the temperature fluctuations acquire a quasi-stochastic character resembling thermal noise.

Fig. 3 shows comparison of the analytical solution (bottom) and the computer simulation of the crystal dynamics (top). The crystal under consideration contains 10^3 particles. The analytical solution is described by formula (9) or (17). The computer simulation uses the method of central differences to solve numerically the system of 10^3 differential equations of the chain dynamics (1) with the integration step $0.02/\omega_e$. The results over 100 realizations of such chain with an independent random initiation are averaged. As it can be seen from Fig. 3 the graphs of the computer simulation and the analytical solution are almost identical.

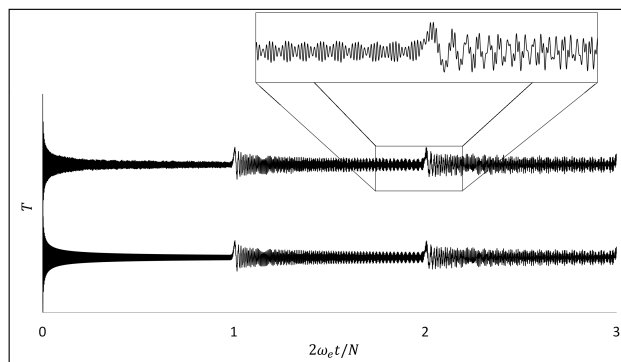


FIG. 3. Oscillations of kinetic temperature T in the finite crystal. Numerical (top) and analytical (bottom) solutions. The averaging is performed using 100 numerical experiments. The number of particles $N = 10^3$, t is time and ω_e is the elementary frequency.

C. Asymptotics

Expression (17), which describes the thermal oscillations in the crystal, includes Bessel functions of multiple orders. In the time-vicinity of the thermal echo appearance the following asymptotic representation of the Bessel functions [41] can be used:

$$J_\mu(x) = \left(\frac{2}{\mu}\right)^{1/3} \text{Ai}\left(\left(\frac{2}{\mu}\right)^{1/3}(\mu - x)\right) + O(\mu^{-1}), \quad (23)$$

where Ai is the Airy function [?] [41]. This representation is valid [?] for $x \approx \mu \gg 1$. More general asymptotics, which is valid for any x is given in Appendix D. The important advantage of these asymptotic representations is that they express special function $J_\mu(x)$ of two variables x, μ in terms of a special Airy function of a single variable. Therefore each thermal mode (22) except the basic mode can be obtained from the Airy function by a linear transformation. The Airy function graph in a form of $\text{Ai}(-z)$ is depicted in Fig. 4. This graph demonstrates the shape of the thermal echo in the thermodynamic limit ($N \rightarrow \infty$), where the value $z = 0$ corresponds to the reference time $t = p\tau_0$ of the thermal echo number p . It is a bit unexpected, that the significant temperature increase starts before the reference time, that is before the long waves from the initial disturbance formally meet each other. Probably this is due to the nature of discrete systems, where some energy can be transferred faster than the speed of sound of the corresponding continuum system.

Then the temperature (17) can be represented as

$$T \approx T_E + \frac{\Delta T}{2} J_0(4\omega_e t) + \Delta T \sum_{p=1}^{\infty} \frac{1}{\sqrt[3]{pN}} \text{Ai}\left(\frac{2pN - 4\omega_e t}{\sqrt[3]{pN}}\right). \quad (24)$$

For large values of arguments $x \gg \mu + 1$ the following asymptotics for the Bessel functions fulfils [41]:

$$J_\mu(x) = \sqrt{\frac{2}{\pi x}} \cos\left(x - \frac{\pi\mu}{2} - \frac{\pi}{4}\right) + O(x^{-2}). \quad (25)$$

Asymptotic representations (23) and (25) for the Bessel functions allows to obtain the basic characteristics of the temperature oscillations for large N .

D. Characteristics of thermal echo

Let us consider the thermal mode number p :

$$T_p = \nu_p \Delta T J_{2pN}(4\omega_e t) \quad (26)$$

for large values of N , where $\nu_p = \frac{1}{2}$ for $p = 0$ (the basic thermal mode) and $\nu_p = 1$ otherwise.

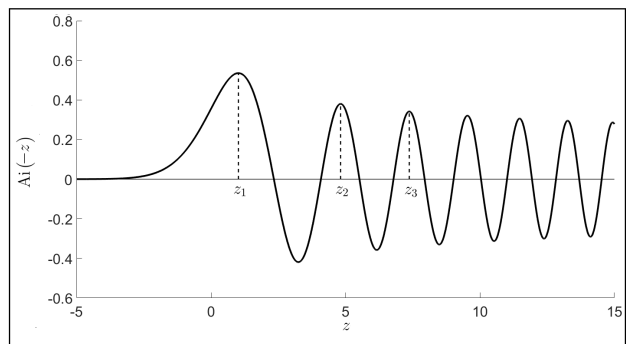


FIG. 4. The Airy function. Such a form takes any thermal echo for a sufficiently large number of particles N .

In the vicinity of the reference time $t = p\tau_0$ the thermal mode T_p with the use of asymptotics (23) can be represented as

$$T_p \simeq \frac{\nu_p \Delta T}{\sqrt[3]{pN}} \text{Ai}\left(\frac{2pN - 4\omega_e t}{\sqrt[3]{pN}}\right). \quad (27)$$

The Airy function $\text{Ai}(-z)$ is depicted in Fig. 4. Let z_k be the successive points of the local maximums of this function, where $k = 1, 2, 3, \dots$ is the point number; $A_k \stackrel{\text{def}}{=} \text{Ai}(-z_k)$ are the corresponding maximums of the function. The first three values of these constants are [46]:

$$\begin{aligned} z_1 \approx 1.0 : \quad A_1 \approx 0.53, \\ z_2 \approx 4.8 : \quad A_2 \approx 0.38, \\ z_3 \approx 7.4 : \quad A_3 \approx 0.34. \end{aligned} \quad (28)$$

Then the corresponding points of the first local maximums t_p and the maximum values M_p for the thermal mode (27) are

$$t_p \simeq \frac{1}{4\omega_e} \left(2pN + \sqrt[3]{pN}\right), \quad M_p \simeq \frac{\nu_p \Delta T}{\sqrt[3]{pN}} A_1. \quad (29)$$

The formula for t_p can be rewritten in the form

$$t_p \simeq p\tau_0 \left(1 + \frac{1}{2(pN)^{2/3}}\right). \quad (30)$$

Hence the relative difference between the reference time and the time of the temperature maximum t_p decreases with increase of N , which proves that these times coincide in the continuum limit.

In the vicinity of the reference time $t = p\tau_0$ the previous thermal mode T_{p-1} (26) with the use of asymptotics (25) can be represented as

$$T_{p-1} \simeq (-1)^N \nu_{p-1} \frac{\Delta T}{\sqrt{\pi N p}} \cos\left(4\omega_e t - \pi N p - \frac{\pi}{4}\right). \quad (31)$$

Let us define the relative height of the thermal echo h_p as a ratio of the maximum value of the thermal mode

number p (29) to the amplitude of the residual oscillations from the previous thermal mode (31), which gives [?]

$$h_p \simeq \frac{\sqrt{\pi} A_1 \sqrt[6]{pN}}{\nu_{p-1}}. \quad (32)$$

Thus the relative height of the thermal echo h_p increases with increasing N . Therefore for very large N the residual oscillations can be considered as negligible. However this increase is very slow — proportional to $N^{1/6}$, hence even for $N = 10^6$ the residual oscillations are quite noticeable.

To analyze the thermal echo properties let us introduce its relative width w_k as the ratio of the quasiperiod of the corresponding Bessel function to the asymptotic period of Bessel functions at infinity. From formulas (23)–(25) it follows that the relative width is proportional to $N^{1/3}$ (see appendix E):

$$w_k \simeq \frac{z_{k+1} - z_k}{2\pi} \sqrt[3]{pN}. \quad (33)$$

From relations (32) and (33) it follows that for large N the residual oscillations from the previous thermal echo are small and frequent in comparison with the current thermal echo wave — see Fig. 2.

E. Example

As an example let us consider a chain of $N = 10^3$ carbon atoms forming a ring with the initial temperature $T_0 = 0^\circ\text{C}$. The heat perturbation instantaneously increases the temperature up to the value

$$T_0 + \Delta T = 100^\circ\text{C}. \quad (34)$$

The chosen value of ΔT is sufficiently small in comparison with the melting temperature of carbon (3500°C), so as not to take into account the nonlinearity of the interatomic interaction. As a result of this perturbation the temperature oscillations near the equilibrium value of $T_E \approx 50^\circ\text{C}$ are realized in the crystal. The graph of the temperature oscillations for the crystal calculated using numeric and analytical solution is shown in Fig. 3. Formula (29) gives for the maximum value of the first thermal mode

$$M_1 \approx 5.3^\circ\text{C} \quad \Longrightarrow \quad T_E + M_1 \approx 55.3^\circ\text{C}. \quad (35)$$

Thus the thermal echo brings approximately 10% change of the temperature comparing to the final temperature raise $T_E - T_0 \approx 50^\circ\text{C}$.

These results are slightly perturbed by the residual oscillations from the previous (the basic) thermal mode. Formulas (32) and (33) yield

$$h_1 \approx 5.9, \quad w_1 \approx 11.3, \quad (36)$$

hence the residual oscillations are approximately 6 times weaker and have 11 times shorter period than the oscillations caused by the first thermal echo. The residual oscillations according to formula (31) have the amplitude of approximately 0.9°C , which is about 17% of M_1 . If the residual oscillations are taken into account the maximum temperature achieved by the first thermal echo is approximately 56.2°C .

The above characteristics depend only on the number of particles N , while the period τ_0 of the thermal echo realization depends on the physical properties of the crystal and the type of oscillations (longitudinal or transversal). Let us consider longitudinal oscillations, the mass of the carbon atom $m = 1.99 \cdot 10^{-26}$ kg and the stiffness of diamond bond $C = 1824$ N/m [47]. Then formula (21) gives $\tau_0 = 1.65 \cdot 10^{-12}$ s that is a $\frac{N}{4\pi} \approx 80$ times greater than the atomic oscillation period.

The obtained numeric characteristics of the thermal echo can be used to determine its occurrence in natural experiments.

IV. CONCLUSIONS

The paper considers a finite one-dimensional harmonic crystal subjected to an instant spatially uniform thermal perturbation. The numeric and analytical analysis presented in the paper demonstrates the phenomenon of the thermal echo: a sharp short-term temperature rise that is periodically realized in the crystals.

Previous papers [26, 33] have shown that in the infinite harmonic crystal the instant thermal perturbation produces the thermal oscillations with a monotonically decreasing amplitude, these oscillations are described by the zero order Bessel function. In the present paper it is shown that in the finite harmonic crystal the sequence of realizations of the thermal echo is described by a series of the Bessel functions of multiple orders. Any thermal echo in the thermodynamic limit is described by the Airy function. A superposition of the temperature oscillations generated by the sequential thermal echoes results in a temperature beats. Each subsequent thermal echo complicates the shape of the beats.

It follows thus from the analysis that the maximum temperature increase caused by the thermal echo decreases as $\sqrt[3]{pN}$ (29), where p the thermal echo number and N is the number of particles in the crystal. The width of the thermal echo grows by the same law (33). Between any two thermal echoes the amplitude of the temperature oscillations decreases in proportion to the square root of time (25). The larger is the crystal, the more noticeable are the temperature increases against the residual oscillations (32).

Thus, an analytical description of the phenomenon of the thermal echo is presented. This phenomenon is an important feature of thermal processes in finite systems and should be taken into account in the development of the modern micro- and nanosize electronic devices.

ACKNOWLEDGMENTS

The authors would like to express their sincere gratitude to W.G. Hoover, D.A. Indeitsev and V.A. Kuzkin for their time and useful discussions.

This work was supported by the Russian Science Foundation (grant 18-11-00201).

APPENDIXES

Appendix A: The initial problem for the velocities covariance

Let us consider displacements covariance and velocities covariance:

$$\xi_n = \langle u_k u_{k+n} \rangle, \quad \kappa_n = \langle v_k v_{k+n} \rangle, \quad (\text{A1})$$

where \mathcal{L} the operator from the problem (1). Differentiation of expression (A1) gives us the equation

$$\dot{\kappa}_n = \mathcal{L}\dot{\xi}_n, \quad (\text{A2})$$

that leads us to the conservation law:

$$\kappa_n - \mathcal{L}\xi_n = \epsilon_n^0, \quad (\text{A3})$$

where the constant ϵ_n^0 can be obtained from the initial conditions (3):

$$\epsilon_n^0 = \kappa_n \Big|_{t=0} = \sigma^2 \langle \tilde{\rho}_k \tilde{\rho}_{k+n} \rangle \Big|_{t=0}, \quad (\text{A4})$$

where $\tilde{\rho}_k$ is centered random numbers. Let us consider the following expression:

$$\langle \tilde{\rho}_k \tilde{\rho}_{k+n} \rangle = \langle \rho_k \rho_{k+n} \rangle - 2\langle \rho_k \bar{\rho} \rangle + \langle \bar{\rho}^2 \rangle, \quad (\text{A5})$$

where $\bar{\rho}$ is the mean value of ρ_k . Let us take into account that

$$t=0: \quad \langle \rho_k \bar{\rho} \rangle = \frac{\rho_k}{N} \sum_{n=0}^{N-1} \rho_{k+n} = \frac{1}{N}, \quad \bar{\rho}^2 = \frac{1}{N}, \quad (\text{A6})$$

then

$$\epsilon_n^0 = \sigma^2 \delta_n - \frac{\sigma^2}{N}. \quad (\text{A7})$$

The equations below can be obtained by differentiating twice (A1):

$$\ddot{\xi}_n = 2(\kappa_n + \mathcal{L}\xi_n), \quad \ddot{\kappa}_n = 2\mathcal{L}(\kappa_n + \mathcal{L}\xi_n). \quad (\text{A8})$$

The use of conservation law (A3) gives us a closed equation for each covariance:

$$\ddot{\xi}_n - 4\mathcal{L}\xi_n = 2\mathcal{L}\epsilon_n^0, \quad \ddot{\kappa}_n - 4\mathcal{L}\kappa_n = -2\mathcal{L}\epsilon_n^0. \quad (\text{A9})$$

The second equation of (A9) and (A4) gives us the initial problem for κ_n .

Appendix B: Equation for velocities covariances

Let us consider the initial problem (7) with the corresponding boundary conditions:

$$\begin{aligned} \ddot{\kappa}_n - 4\mathcal{L}\kappa_n &= -2\sigma^2 \mathcal{L}\delta_n, \\ t=0: \quad \kappa_n &= \sigma^2 \delta_n - \frac{\sigma^2}{N}, \quad \dot{\kappa}_n = 0, \\ \kappa_0 &= \kappa_N, \quad \kappa_{N+1} = \kappa_1. \end{aligned} \quad (\text{B1})$$

Then we apply the discrete Fourier transformation

$$\kappa_k^* = \sum_{n=0}^{N-1} \kappa_n e^{-\frac{2\pi i k n}{N}} \quad (\text{B2})$$

to the initial problem (B1):

$$\begin{aligned} \ddot{\tilde{\kappa}}_k + 4\mathbb{L}\tilde{\kappa}_k &= 0, \\ t=0: \quad \tilde{\kappa}_k &= \frac{\sigma^2}{2} - \sigma^2 \delta_k, \quad \dot{\tilde{\kappa}}_k = 0, \end{aligned} \quad (\text{B3})$$

where

$$\tilde{\kappa}_k = \kappa_k^* - \frac{\sigma^2}{2}, \quad \mathbb{L} = 4\omega_e^2 \sin^2 \frac{\pi k}{N}. \quad (\text{B4})$$

The solution of the problem (B3) is

$$\tilde{\kappa}_k = \frac{\sigma^2}{2} (1 - 2\delta_k) \cos \left(4\omega_e t \sin \frac{\pi k}{N} \right), \quad (\text{B5})$$

hence

$$\kappa_k^* = \frac{\sigma^2}{2} \left[(1 - 2\delta_k) \cos \left(4\omega_e t \sin \frac{\pi k}{N} \right) + 1 \right]. \quad (\text{B6})$$

The inverse Fourier transform for κ_k^* is

$$\begin{aligned} \kappa_n &= \\ \frac{1}{N} \frac{\sigma^2}{2} \sum_{k=0}^{N-1} \left(1 + \cos \left(4\omega_e t \sin \frac{\pi k}{N} \right) \right) e^{i \frac{2\pi n k}{N}} &- \frac{\sigma^2}{N}. \end{aligned} \quad (\text{B7})$$

The $\kappa_n|_{n=0}$ which is proportional ΔT is

$$\kappa_n|_{n=0} = \frac{\sigma^2}{2} \left(1 + \frac{1}{N} \sum_{k=1}^{N-1} \cos \left(4\omega_e t \sin \frac{\pi k}{N} \right) \right). \quad (\text{B8})$$

Appendix C: The formula for the sum of cosines of multiple angles

Let us demonstrate that the sum of the multiple angles of the cosine can be represented by the following form:

$$\frac{1}{N} \sum_{k=0}^{N-1} \cos \left(p \frac{2\pi k}{N} \right) = \frac{\sin(2\pi p)}{2N} \operatorname{ctg} \frac{\pi p}{N} + \frac{\sin^2(\pi p)}{N}. \quad (\text{C1})$$

The sum of cosines of multiple angles can be calculated as a sum of exponentials, which is calculated as the sum of the geometric progression:

$$\sum_{k=1}^{N-1} \cos k\phi = \operatorname{Re} \sum_{k=1}^{N-1} e^{ik\phi} = \operatorname{Re} \left(\frac{e^{iN\phi} - e^{i\phi}}{e^{i\phi} - 1} \right). \quad (\text{C2})$$

Calculation of the real part (C2) gives us one of the following representations:

$$\begin{aligned} \sum_{k=0}^{N-1} \cos k\phi &= \\ \frac{\sin(N\phi - \phi/2)}{2 \sin(\phi/2)} - \frac{1}{2} &= \frac{\cos(N\phi/2) \sin((N-1)\phi/2)}{\sin(\phi/2)} = \\ &= \frac{1}{2} \sin(N\phi) \operatorname{ctg}(\phi/2) - \cos^2(N\phi/2). \end{aligned} \quad (\text{C3})$$

For sum

$$F_N(p) \stackrel{\text{def}}{=} \frac{1}{N} \sum_{k=1}^{N-1} \cos \left(p \frac{2\pi k}{N} \right) \quad (\text{C4})$$

we get the following representation:

$$F_N(p) = \frac{\sin(2\pi p)}{2N} \operatorname{ctg} \frac{\pi p}{N} + \frac{\cos^2(\pi p)}{N}. \quad (\text{C5})$$

For all p , except p that divides by N , the expression $F_N(p)$ from (C5) is equal to $1 - 1/N$, and for p divides by N , the value of the expression $F_N(p)$ is found from (C4), and is equal to $-1/N$.

Appendix D: Asymptotics for the Bessel functions

An asymptotic for the Bessel functions of large orders μ and arbitrary argument x is represented by the series 9.3.35 from [41]. The first term of this expression can be represented as the following composition:

$$J_\mu(x) \simeq \left(\frac{4\zeta}{1-\xi^2} \right)^{1/4} \frac{\operatorname{Ai}(\mu^{2/3}\zeta)}{\mu^{1/3}}, \quad \mu \rightarrow \infty, \quad (\text{D1})$$

where

$$\xi = \frac{x}{\mu} \quad \zeta = \begin{cases} \left(\frac{3}{2} \right)^{2/3} \left[\ln \left(\frac{1 + \sqrt{1 - \xi^2}}{\xi} \right) - \sqrt{1 - \xi^2} \right]^{2/3}, & \text{if } 0 \leq \xi \leq 1; \\ - \left(\frac{3}{2} \right)^{2/3} \left[\sqrt{\xi^2 - 1} - \operatorname{arcsec} \xi \right]^{2/3}, & \text{if } \xi \geq 1, \end{cases}$$

and Ai is the Airy function [41].

In the case of the $\xi \rightarrow 1$, the representation (D1) is reduced to the following one:

$$J_\mu(x) \approx \left(\frac{2}{\mu} \right)^{1/3} \operatorname{Ai} \left(2^{1/3} \mu^{2/3} (1 - \xi) \right), \quad (\text{D2})$$

where the approximation $\zeta \approx 2^{1/3}(\xi - 1)$ is used. The (D2) is equivalent to representation (23), considered before.

Appendix E: Relative width of the thermal echo

Let us denote by $\{x_i\}$ the set of points in which the Bessel function $J_\mu(x)$ has local maxima (x_1 is the first local maximum, x_2 is the second, etc.). The approximate values of x_i are found from the condition that the argument of the Airy function in the expression (23) is equal to the values $-z_i$ (28):

$$x_i \approx \mu + z_i \left(\frac{\mu}{2} \right)^{1/3}, \quad J_\mu(x_i) \approx \left(\frac{\mu}{2} \right)^{-1/3} \operatorname{Ai}(-z_i). \quad (\text{E1})$$

The value of the asymptotic period of the Bessel function is 2π as seen from the formula (25). Then the expression for the width of the thermal echo becomes:

$$w_i \stackrel{\text{def}}{=} \frac{x_{i+1} - x_i}{2\pi} \approx \frac{z_{i+1} - z_i}{2\pi} \left(\frac{\mu}{2} \right)^{1/3}. \quad (\text{E2})$$

-
- [1] Rieder, Z., Lebowitz, J.L., Lieb, E. Properties of a Harmonic Crystal in a Stationary Nonequilibrium State. *J. Math. Phys.* **8**, 5 (1967).
- [2] Gendelman, O.V., Savin, A.V. Normal Conductivity of the One-Dimensional Lattice with Periodic Potential of Nearest-Neighbor Interaction. *Phys. Rev. Lett.* **84**, 11 (2000).
- [3] Krivtsov, A.M. Heat transfer in infinite harmonic one dimensional crystals. *Doklady Physics* **60**, 9 (2015).
- [4] Kuzkin, V.A., Krivtsov, A.M. An analytical description of transient thermal processes in harmonic crystals. *Physics of the Solid State* **59**, 5 (2017).
- [5] Lepri, S., Livi, R., Politi, A. Thermal conduction in classical low-dimensional lattices. *Phys. Rep.* **377**, 1 (2003).
- [6] Chang, C.W., Okawa, D., Garcia, H., Majumdar, A., Zettl, A. Breakdown of Fourier's Law in Nanotube Thermal Conductors. *Phys. Rev. Lett.* **101**, 075903 (2008).
- [7] Guzev, M.A., Dmitriev, A.A. . Oscillatory-damping temperature behavior in one-dimensional harmonic model of a perfect crystal. *Dal'nevost. Mat. Zh.* **17**, 2 (2017)
- [8] Bonetto, F., Lebowitz, J.L., Rey-Bellet, L. Fourier's law: a challenge to theorists. In: Fokas, A., Grigoryan, A., Kibble, T., Zegarlinski, B. (eds.). *Mathematical Physics 2000*. World Scientific, Singapore (2000)
- [9] Hsiao, T.,K., Huang, B.W., Chang, H.K., Liou, S.C., Chu, M.W., Lee, S.C., Chang, C.W. Micron-scale ballistic thermal conduction and suppressed thermal conductivity in heterogeneously interfaced nanowires. *Phys. Rev. B* **91** 3, 035,406 (2015)
- [10] Kanel, G.I., Razorenov, S.V., Utkin, A.V., Fortov, V.E. Shock-wave phenomena in condensed media. *Yanus-K, Moscow*. (1996) 407 p. (in Russian)
- [11] Holian, B.L., Hoover, W.G., Moran, B., Straub, G.K. Shock-wave structure via nonequilibrium molecular dynamics and Navier-Stokes continuum mechanics. *Phys. Rev. A* **22**, 2798 (1980).
- [12] Holian, B.L., Mareschal, M. Heat-flow equation motivated by the ideal-gas shock wave. *Phys. Rev. E* **82**, 026707 (2010).
- [13] Hoover, W.G., Hoover, C.G., Travis, K.P. Shock-wave compression and Joule-Thomson expansion. *Phys. Rev. Lett.* **112**, 144504 (2014).
- [14] Silva, F., Teichmann, S.M., Cousin, S.L., Hemmer, M., Biegert, J. Spatiotemporal isolation of attosecond soft X-ray pulses in the water window. *Nat. Commun.* **6**, 6611 (2015).
- [15] Ashitkov, S. I., Komarov, P.S., Agranat, M.B., Kanel, G.I., Fortov, V.E. Achievement of ultimate values of the bulk and shear strengths of iron irradiated by femtosecond laser pulses. *JETP Letters* **98**, 7 (2013).
- [16] Inogamov, N.A., Petrov, Yu.V., Zhakhovsky, V.V., Khokhlov, V.A., Demaske, B.J., Ashitkov, S.I., Khishchenko, K.V., Migdal, K.P., Agranat, M.B., Anisimov, S.I., Fortov, V.E., Oleynik, I.I. Two-temperature thermodynamic and kinetic properties of transition metals irradiated by femtosecond lasers. *AIP Conf. Proc.*, **1464**, 593 (2012).
- [17] Poletkin, K.V., Gurzadyan, G.G., Shang, J., Kulish, V. Ultrafast heat transfer on nanoscale in thin gold films. *Applied Physics B* **107**, 137 (2012).
- [18] Bykovsky, N.E., Zavedeev, E.V., Ralchenko, V.G., Senatsky, Y.V. Surface damage of YAG crystal induced by broadband nanosecond laser pulses: Morphology of craters and material deformation *Laser Physics Letters*, **12**, 5 (2015).
- [19] Indeitsev, D.A., Naumov, V.N., Semenov, B.N., Belyaev, A.K. Thermoelastic waves in a continuum with complex structure. *ZAMM-Z. Angew. Math. Mech.*, **89**, 279 (2009).
- [20] Indeitsev, D.A., Osipova, E.V. A two-temperature model of optical excitation of acoustic waves in conductors. *Doklady Physics*, **62**, 3 (2017).
- [21] Saadatmand, D., Xiong, D., Kuzkin, V.A., Krivtsov, A.M., Savin, A.V., Dmitriev, S.V. Discrete breathers assist energy transfer to ac-driven nonlinear chains. *Phys. Rev. E*, **97**, 2, 022217, (2018).
- [22] Guzev, M.A., Dmitriev, A.A. Different representations for solving one-dimensional harmonic model of a crystal. *Dal'nevost. Mat. Zh.* **17**, 1 (2017).
- [23] Gendelman, O.V, Savin, A.V. Nonstationary heat conduction in one-dimensional chains with conserved momentum. *Phys. Rev. E* **81**(2), 020,103 (2010).
- [24] Babenkov, M.B., Krivtsov, A.M., Tsvetkov, D.V. Energy oscillations in a one-dimensional harmonic crystal on an elastic substrate. *Physical Mesomechanics*, **19**, 3 (2016).
- [25] Shishkina, E.V., Gavrilov, S.N. A strain-softening bar with rehardening revisited. *Math. Mech. Solids* **21**(2), 137151 (2016).
- [26] Krivtsov, A.M. Energy oscillations in a one-dimensional crystal. *Doklady Physics*, **59**, 9 (2014).
- [27] Krivtsov, A.M. On unsteady heat conduction in a harmonic crystal. *arXiv:1509.02506* (2015).
- [28] Gavrilov, S.N., Krivtsov, A.M., Tsvetkov, D.V. Heat transfer in a one-dimensional harmonic crystal in a viscous environment subjected to an external heat supply. *Continuum Mech. Thermodyn.* (2018).
- [29] Kuzkin, V.A., Krivtsov, A.M. High-frequency thermal processes in harmonic crystals. *Doklady Physics* **62**, 2, (2017).
- [30] Kuzkin, V.A., Krivtsov, A.M. Fast and slow thermal processes in harmonic scalar lattices. *Journal of Physics: Condensed Matter* **29** (50), 505401, (2017).
- [31] Tsaplin, V.A., Kuzkin, V.A. Temperature oscillations in harmonic triangular lattice with random initial velocities. *Letters on Materials*, **8**, 1, pp. 16-20, (2018).
- [32] Allen, M.P., Tildesley, A.K. *Computer Simulation of Liquids*. Clarendon Press, Oxford. (1987). 390 p.
- [33] Klein, G., Prigogine, I. Sur la mecanique statistique des phenomenes irreversibles. *Physica* **19**, 1053 (1953).
- [34] Krivtsov, A.M., Murachev, A.S., Tsvetkov, D.V. Non-stationary thermodiffusion processes in a finite one-dimensional crystal. *Chebyshevskii Sbornik*, **18**, 3, (2017) (in Russian).
- [35] Goldstein, R.V., Morozov, N.F. Mechanics of deformation and fracture of nanomaterials and nanotechnology. *Physical Mesomechanics* **10** 5-6 (2007).
- [36] Golovnev, I.F., Golovneva, E.I., Fomin, V.M. The influence of a nanocrystal size on the results of molecular-dynamics modeling. *Comp. Mat. Sci.* **36**, 176 (2006).
- [37] Korobeynikov, S.N., Alyokhin, V.V., Annin, B.D.,

- Babichev, A. V. Using Stability Analysis of Discrete Elastic Systems to Study the Buckling of Nanostructures. *Archives of Mechanics*. **64**, 367 (2012).
- [38] Krivtsov, A. M., Morozov, N. F. On mechanical characteristics of nanocrystals. *Physics of the Solid State* **44**, 12 (2002).
- [39] Baimova, Y. A., Murzaev, R. T., Dmitriev, S. V. Document Mechanical properties of bulk carbon nanomaterials *Physics of the Solid State* **56**, 10 (2014).
- [40] Dhar, A., Dandekar, R. Heat transport and current fluctuations in harmonic crystals. *Phys. A*, **418**, 49 (2014).
- [41] Abramowitz, M. and Stegun, I. A. *Handbook of Mathematical Functions With Formulas, Graphs, and Mathematical Tables*. New York: Dover. (1964). 1046 p.
- [42] *Mathematical Encyclopedia*. Ed. I. M. Vinogradov. A-G. Soviet Encyclopedia, Moscow. (1982). 5500 p.
- [43] Hoover, W.G., Hoover, C.G. *Simulation and Control of Chaotic Nonequilibrium Systems: Advanced Series in Nonlinear Dynamics: V. 27*. World Scientific, Singapore. (2015). 324 p.
- [44] Born, M., and Huang, K. *Dynamical Theory of Crystal Lattices*. Oxford University Press, London and New York (1954).
- [45] Krivtsov, A.M., Kuzkin, V.A. Discrete and continuum thermomechanics. *Encyclopedia of Continuum Mechanics* (2018).
- [46] Fabijonas, B.R., Olver, F.W.J. On the reversion of an asymptotic expansion and the zeros of the Airy functions. *SIAM Rev.* **41**, 762 (1999).
- [47] Berinskii, I.E., Krivtsov, A.M. A hyperboloid structure as a mechanical model of the carbon bond. *International Journal of Solids and Structures*. **96**, 152 (2016).